Quantum Signature Blurred by Disorder in Indirect Exciton Gases

Mathieu Alloing[1], Aristide Lemaître[2], François Dubin[1]
[1] *ICFO-Institut de Ciències Fotòniques, Mediterranean Technology Park, Av. del Canal Olímpic, E-08860 Castelldefels, Spain and*
[2] *Laboratoire de Photonique et Nanostructures, LPN/CNRS, Route de Nozay, 91460 Marcoussis, France*
(Dated: January 6, 2011)

The photoluminescence dynamics of a microscopic gas of indirect excitons trapped in coupled quantum wells is probed at very low bath temperature (≈ 350 mK). Our experiments reveal the non linear energy relaxation characteristics of indirect excitons. Particularly, we observe that the excitons dynamics is strongly correlated with the screening of structural disorder by repulsive exciton-exciton interactions. For our experiments where two-dimensional excitonic states are gradually defined, the distinctive enhancement of the exciton scattering rate towards lowest energy states with increasing density does not reveal unambiguously quantum statistical effects such as Bose stimulation.

PACS numbers: 78.67.De, 73.63.Hs

The development of trapping and cooling techniques of atomic gases has lead to major advances in the studies of quantum matter. For bosonic atoms, a striking example is given by the Bose stimulation towards occupation of the system ground-state. This manifests that quantum statistics is dominant and triggers the subsequent Bose-Einstein condensation [1]. At present, atomic condensates are routinely produced to investigate further many-body quantum states [2], and signatures observed with these shall constitute milestones to demonstrate Bose-Einstein condensation of any bosonic system.

In the solid-state, a variety of quasi-particles with bosonic character can also be found. Particularly, semiconductors exhibit bound electron-hole pairs called excitons, as well as (exciton-)polaritons which correspond to the coherent superposition of photonic and excitonic degrees of freedom. For the latter composite states, Bose amplification induced by stimulated energy relaxation was reported [3–5], followed by the observation of polaritons condensation [6–8]. On the other hand, signatures of Bose-Einstein statistics for excitons are controversial [9], however, quantum signatures such as macroscopic coherence have been reported [10, 11].

In the quest for exciton condensation, bilayer semiconductor heterostructures were introduced [12] and have resulted in significant achievements towards observation of quantum statistics of exciton many-body states. A notable example is given by devices where a double quantum well (DQW) is embedded in a Schottky junction [13, 14]. The latter is used to control the electric field in the structure such that excitons are rendered indirect, i.e. that electrons and holes are each confined in a distinct quantum well. This situation yields important advantages: Mostly, the spatial overlap between the electron and hole wave-functions is greatly reduced which leads to long lived excitonic states, from tens of nanoseconds to microseconds timescales. On the other hand excitons can relax with a (sub-)nanosecond dynamics close to the lattice temperature. In addition, excitons are electrically polarized with well aligned electric dipoles which induces strong exciton-exciton repulsions limiting ionization at low temperature.

Recently, DQW structures have been utilized to implement electrostatic traps for indirect excitons. These are based on micro-patterned gate electrodes [15–17] which allow one to confine an exciton gas in a microscopic region. In the past years, the exciton trap technology has rapidly evolved [18–20] and a set of phenomena expected for exciton condensates have been observed, e.g. the appearance of macroscopic coherence across an exciton gas along with a spectral narrowing and linear polarization of the fluorescence emission [11]. Nevertheless, direct evidences for the quantum statistics of excitons have not been reported in exciton traps yet.

The photoluminescence dynamics of indirect excitons holds essential informations to identify signatures of many-body quantum states. This was well illustrated in studies of macroscopic gases which have revealed a sharp enhancement (or "jump") of the photoluminescence signal once the external laser excitation creating excitons is switched off [21]. In fact, in a regime free from external heating source, indirect excitons experience a fast relaxation towards lowest energy states which leads to a high occupation of the excitonic ground state. Furthermore, the photoluminescence enhancement occurs at a rate which increases with the exciton concentration such that it was interpreted as a signature of stimulated exciton scattering [22]. However, theoretical analysis following these observations stressed the role that disorder can play in the increase of the photoluminescence enhancement as a function of the density [23].

In this letter, we study experimentally the mutual influence of disorder and repulsive exciton-exciton interactions in the photoluminescence dynamics of indirect excitons. We probe a microscopic trap in which indirect excitons are created by non resonant pulsed excitation. Besides revealing the photoluminescence enhancement characteristics of indirect excitons, our experiments point out strong correlations between the excitons dynamics and the screening of disorder by repulsive exciton-exciton interactions. As the exciton concentration is increased, repulsive dipolar interactions induce a diffusion of excitons

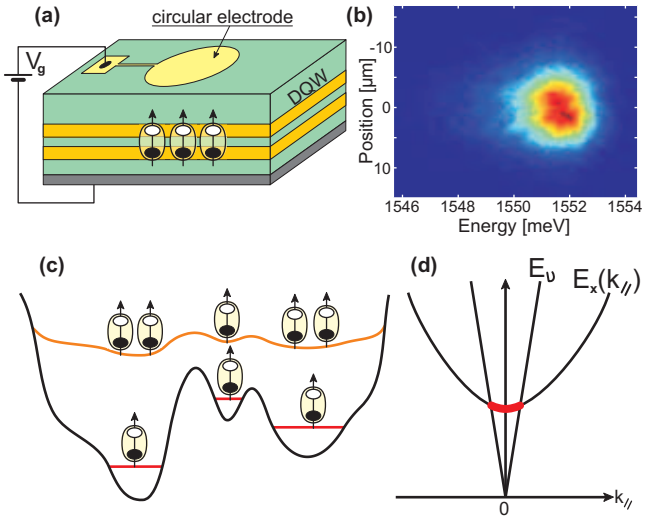

FIG. 1: (Color Online) (a): Schematic representation of the electrostatic trap. Electrons and holes are displayed by filled and open circles respectively while the arrows indicate the excitons electric dipole. (b): Spatially resolved emission spectrum of indirect excitons recordered in a 10 ns window at low density ($n_{2D} \approx 10^9$ cm^{-2}) and T_b= 360 mK. (c): Cartoon depiction of disorder screening induced by repulsive dipole interactions: At low densities, excitons occupy minima of the random potential while at higher densities the excitonic diffusion leads to a smooth in-plane effective potential, i.e. that inhomogenous broadening is largely suppressed. (d) Excitons and photons energy dispersion, E_X and E_ν respectively. Bright exciton states, i.e. those yielding photo-emission, are marked in bold.

which become delocalized as marked by a spectral narrowing of the photoluminescence emission. Accordingly, a clear boundary is gradually induced between optically active and inactive exciton states that governs the magnitude of photoluminescence enhancement [23]. In that context, we conclude that the excitons quantum statistics is not unambiguously signaled.

As shown schematically in Fig. 1.a, we study an electrostatic trap for indirect excitons which is generated by a semitransparent disk-shape gate electrode of 100 μm diameter. A DQW consisting of two 8 nm wide GaAs quantum wells separated by a 4 nm $Al_{0.33}Ga_{0.67}As$ barrier is positioned 950 nm under the gate electrode and 50 nm above a bottom GaAs substrate rendered homogeneously conductive by Si-doping ($n_{Si} \approx 10^{18}$ cm^{-3}). This design hence fulfills requirements for a stable trapping of a high-density exciton gas [24]. The semiconductor sample is placed on the He^3 insert of a He^4 optical cryostat which allows us to perform microscopy at low bath temperature ($T_b \geq 350$ mK). In the following experiments, a constant bias V_g= 1.33 V is applied to the gate electrode such that the excitonic ground state is of indirect type with holes confined in the top quantum well and electrons in the lower one (see Fig. 1.a). The electrostatic trap is imaged utilizing an aspherical lens, of numerical aperture NA=0.6, which is positioned by piezo-electric transducers inside the cryostat in a configuration where we achieve an overall spatial resolution of $\approx$ 1-2 μm. "Hot" indirect excitons are created at the center of the trap after excitation by a defocussed laser at 642 nm, i.e. $\approx$ 0.4 eV above the indirect excitons energy. At the trap surface, the laser excitation exhibits a gaussian spatial profile with 10 μm FWHM. In the following experiments, we utilize 50 ns long laser pulses at a repetition rate of 4 MHz and analyze the variation of the photoluminescence (PL) of indirect excitons as a function of the density. The latter is controlled by the power of laser excitation which we vary from $\approx$ 100 nW to 100 μW. The excitonic fluorescence is finally recorded with an imaging spectrometer coupled to an intensified CCD camera combining 2 ns and 100 μeV temporal and spectral resolution respectively. Figure 1.b displays a spatially resolved emission spectrum recorded at very low excitation power ($\approx$ 100 nW).

As the excitation power increases, the maximum of the photoluminescence shifts towards higher energies. This variation results from the repulsive dipole-dipole interactions between indirect excitons and the energy shift, δE, gives an estimation of the gas density inside the trap [25]. Indeed, the mean field energy associated to repulsive exciton-exciton interactions may be expressed as $U_{\rm rep}$=u_0.n_{2D}, where u_0 is a constant factor controlled by the DQW geometry and the correlations between excitons [26, 27]. For our trap, we estimate that 6 10^9 cm^{-2} $\leq n_{2D} \leq$ 8 10^{10} cm^{-2} for δE = 1 meV which is obtained at an excitation power of $\approx$10μW.

In the regime of low excitonic density, i.e. for $n_{2D} \approx 10^9$ cm^{-2}, we note that indirect excitons remain confined within the region of the trap which is laser excited (see Fig. 2.b). At the same time, the spectral distribution of the emission is rather broad and exhibits a full width at half maximum $\Gamma(0)$=2.70(5) meV (see Fig. 2.a). These observations both indicate that indirect excitons are trapped by the random fraction of the trapping potential, $U_{\rm rand}(r_\parallel)$, $r_\parallel$ denoting the coordinates in the plane of the quantum wells. At the center of the trap, the electrostatic potential generated by the gate electrode is *a priori* constant such that $U_{\rm rand}$ may be governed solely by hetero-interface roughness and in plane fluctuations of the electric field, for instance induced by charged impurities. In the following, we show that exciton interactions allow us to circumvent the limitations imposed by $U_{\rm rand}$.

In Figures 2.c-d, we study the variations of the emission spectral width Γ together with its spatial extension L as a function of δE, i.e. as a function of the exciton concentration. The following regimes can be identified: for $\delta E \leq$ 1 meV (region (i)), Γ decreases abruptly from 2.70(5) meV down to 2.08(5) meV while the spatial extension of the gas remains equal to $\approx$ 10 μm. The spectral narrowing observed in this regime is a consequence of the screening of local disorder by repulsive dipole-dipole interactions. This behavior was predicted theoretically [28, 29]: the exciton confining potential is dressed by $U_{\rm rep}$ which yields an effective in-plane poten-

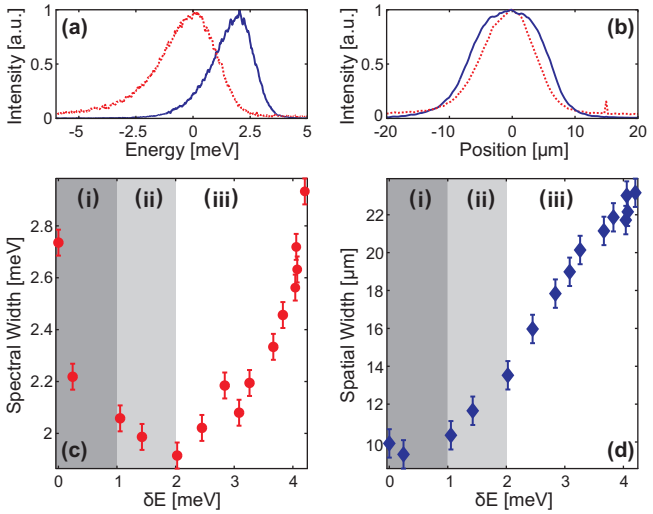

FIG. 2: (Color Online) (a): Emission spectrum averaged in a 20 μm wide region at the center of the trap for δE=0 and 2 meV, dotted and solid lines respectively. The zero in energy is taken at the center of the emission for the lowest exciton density, i.e. for δE=0. (b): Spatial profiles of the emissions shown in (a). (c)-(d): Spectral and spatial emission linewidths as a function of the exciton-exciton repulsive interaction energy δE. Experimental results were recorded in a 10 ns time window and in the same measurements performed at T_b= 360 mK. Error bars display the instrumental resolution.

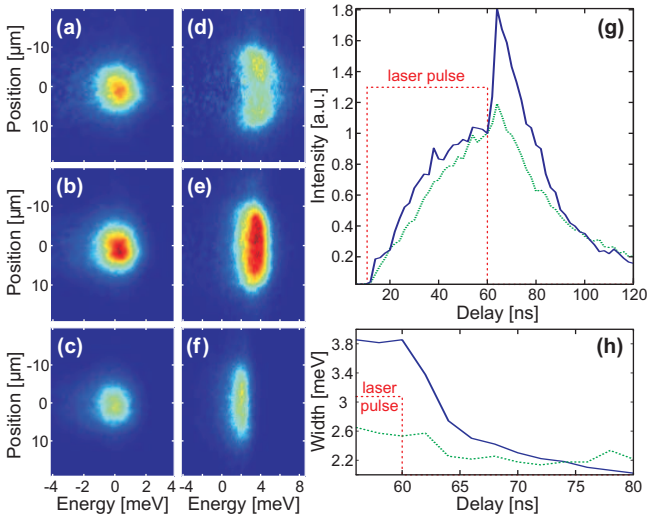

FIG. 3: (Color Online) (a)-(c): Spatially resolved emission spectrum measured at T_b = 400 mK and for δE = 0.25 meV, at the falling edge of the laser pulse (a), and 4 ns and 20 ns later, (b) and (c) respectively. The images were acquired with a 2 ns time window. The energy scale corresponds to the normalized detection energy $E - E(\delta E = 0)$, where $E(\delta E = 0)$ is the energy position of the PL maximum at very low excitation power. (d)-(f): Images recorded in the same experiment as for (a)-(c) but for δE =3.8 meV. (g): Time evolution of the maximum of indirect excitons photoluminescence for δE = 0.25 and 3.8 meV, dotted and solid lines respectively. (h): Time dependence of the spectral linewidth for δE = 0.25 and 3.8 meV, dotted and solid lines respectively.

tial $U_{eff}(r_\parallel) \sim U_{rep}(r_\parallel) + U_{rand}(r_\parallel)$. Thereby, the accumulation of indirect excitons at minima of U_{rand} and the depletion around its maxima smooths the spatial profile of U_{eff} (see Fig.1.c) and the inhomogeneous broadening is locally suppressed. After this regime, i.e. for 1meV $\leq \delta E \leq$ 2meV (region (ii)), we observe that the emission linewidth continues to decrease from 2.10(5) to 1.90(5) meV while the spatial extension of the gas steadily increases from approximately 10 to 14 μm. Hence, the exciton concentration has passed the critical density for which repulsive dipole-dipole interactions are sufficient to drive a macroscopic diffusion. The latter then allows for a screening of disorder correlated at a length scale longer than in region (i). Thereby, the inhomogenous broadening is further reduced and the spatial extension of the cloud rapidly grows since excitons occupy effectively delocalized states in region (ii). Let us note that the variation of the spatial extension of the exciton cloud in region (i)-(ii) is very similar to what observed recently in an electrostatic lattice [19].

In the last region of Fig. 2.c-d, i.e. in region (iii) where 2meV $\leq \delta E \leq$ 4.2 meV, L increases steadily up to 23 μm for $\delta E \approx$ 4 meV, while Γ now increases up to $\sim$3 meV. As shown in previous studies of similar devices [30, 31], the variation of Γ signals a monotonous increase of the homogeneous broadening as the exciton density is increased, in a regime where excitons occupy delocalized states. At the same time, the dipolar pressure is strong for the density range of region (iii) and the exciton cloud hence rapidly expands [32]. In addition, let us note that the highest exciton density which we can estimate [26, 27] remains about an order of magnitude smaller than the critical phase-space filling $(1/a^2)$, a being the exciton Bohr radius. Therefore, exciton dissociation shall not be significant in our experiments, even at large blue shifts as in region (iii) [33]. Finally from the variations of Γ and L presented in Fig. 2.c-d we conclude that a sufficient level of inhomogeneous broadening is required to observe a line narrowing, i.e. a screening of disorder by repulsive exciton interactions (regions (i) and (ii)). In fact, previous studies performed on heterostructures with very low inhomogeneous broadening [30, 31] only revealed variations for Γ which are qualitatively what presented in region (iii) of Fig.2.c.

In the following, we analyze the dynamics of photoluminescence and study the thermalization of indirect excitons: For our experiments performed under non resonant laser excitation, "hot" indirect excitons are injected in the trap, i.e. excitons with an energy $\approx$ 20 meV above the bottom of the energy band. On the other hand, the detected photoluminescence is exclusively due to the recombination of "cold" indirect excitons which have relaxed at the bottom of the energy band, in the optically active region which is restricted to a maximum kinetic energy of $\approx$ 0.1 meV (see Fig. 1.d).

In Figure 3, the spatially and time resolved photoluminescence signal is presented for low and high exciton densities, namely for δE=0.25 and δE = 3.8 meV respectively. Depending on the density, the system exhibits two very different behaviors after the laser excitation is switched off. At low density ($\delta E \sim 0.25$ meV), the linewidth decreases slightly (Fig. 3.h) while the luminescence signal drops rapidly after a small rise (Fig. 3.g). The response to the laser interruption in the high density regime ($\delta E = 3.8$ meV) is far more striking. The linewidth decreases by almost a factor 2 after ∼5 ns while the luminescence signal exhibits a pronounced enhancement (or "jump") by a factor ∼1.8 (Fig. 3.g) within the first nanoseconds. The PL signal then decreases over a few tens of nanoseconds along with a shift towards lower energies (Fig. 3.f). This behavior is very similar to the one observed by Butov *et al.* [21] on macroscopic gases. In general, the drop of the emission linewidth indicates a strong reduction of the effective temperature of the indirect exciton gas once "hot" carriers are not brought anymore into the system. It also reveals a fast thermalization of indirect excitons in the semiconductor matrix, within a few nanosecond timescale. Furthermore, the large enhancement of the photoluminescence marks an important increase of the exciton population in the optically active states. Indeed, theoretical calculations indicate for the experiments displayed in Fig. 3.d-f that the exciton ground state is degenerate [23]. On the other hand, in the dilute regime, though the effective temperature of indirect excitons is reduced, the occupation of bright exciton states is not sufficiently enhanced to induce a significant jump of the PL signal. In fact, the magnitude of the photoluminescence enhancement depends strongly on the exciton density which may be related to Bose stimulation [22].

To identify the relation between quantum statistics and the enhancement of photoluminescence discussed above, we studied in more details the amplitude and the dynamics of the PL jump as a function of δE, i.e. as a function of the exciton density. Experimental results are displayed in Figure 4 and exhibit strong correlations with the variations presented in Figure 2. Indeed, in the high density regime where the heterostructure disorder is efficiently suppressed (region (iii) where $\delta E \geq 2$ meV), the rise time and the magnitude of photoluminescence enhancement barely depend on the exciton density, unlike for Bose stimulation. On the other hand, for lower exciton concentrations the dynamics is far more striking. Precisely, when the mean field energy $U_{\rm rep}$ is not sufficiently large to screen the semiconductor disorder, i.e. in region (i) where $\delta E \leq$ 1meV, we note a steady increase (decrease) of the amplitude (rise time) as a function of the exciton density. Such variations contrast with theoretical works which predict that amplitude and rise time hardly vary with the exciton density in this regime [23]. However, in region (i) excitons are gradually delocalized with increasing $U_{\rm rep}$ such that a well defined energy minimum and density of states are progressively established.

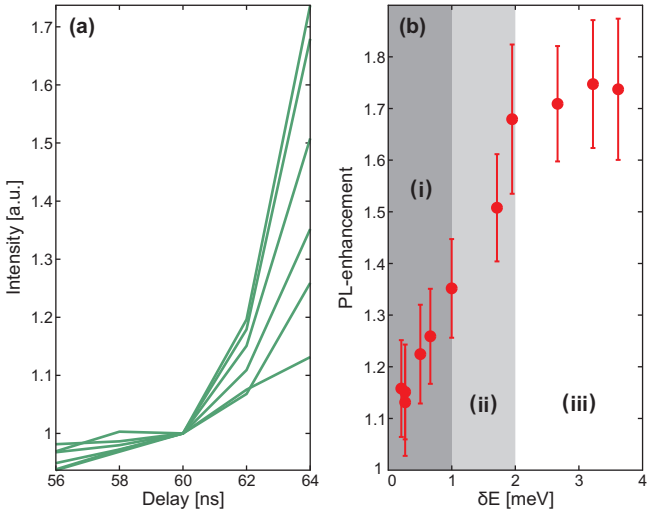

FIG. 4: (Color Online) (a): Time evolution of the photoluminescence enhancement as a function of δE. From bottom to top the curves correspond to δE=0.25-0.65-1-1.7-2-3.6 meV. (b): Magnitude of the photoluminescence enhancement as a function of δE. These results are taken from the same experiment as for Fig. 3 and the regions (i)-(iii) are defined as in Figure 2. Error bars display the Poissonian uncertainty for our measurements.

Hence, a clear distinction between optically active and inactive exciton states is gradually induced. In this context, the PL enhancement is governed by the interplay between the amplitude of disorder and the strength of repulsive exciton interactions which controls the fraction of excitonic states contributing to the photoluminescence emission. On the other hand, the characteristics of the PL jump are more intriguing for intermediate exciton concentrations. Particularly, in region (ii) we note that the magnitude (rise time) of the photoluminescence enhancement increases (decreases) with the exciton density. As shown in Figure 2, excitons occupy delocalized states in this regime such that the influence of disorder can not account for the discrepancy between experimental results and theoretical expectations. Therefore, the increased scattering rate towards low energy states with increasing exciton concentration might reveal bosonic stimulation of exciton scattering in region (ii), as discussed in Ref. [22]. However, the results displayed in Figure 4 show that amplitude and rise time of the PL enhancement exhibit variations in region (i) and (ii) which do not allow us to clearly distinguish regimes where excitons are mostly localized and delocalized respectively. Thereby, the quantum statistics of excitons is not revealed unambiguously.

To summarize, we have studied the photoluminescence dynamics of a microscopic gas of indirect excitons at very low bath temperature. It was shown that repulsive exciton-exciton interactions provide an efficient screening of structural disorder which yields a significant narrowing of the emission spectrum accompanied by a delocalization of indirect excitons. The photoluminescence

dynamics also reveals the interplay between disorder and repulsive dipole interactions between indirect excitons. Particularly, increasing the exciton density, a sharp increase of the photoluminescence signal builds up gradually in a fashion controlled by the efficiency at which disorder is screened in the heterostructure. Though our experiments are carried out under conditions where the exciton ground state is highly occupied, we conclude that direct signatures of Bose statistics are not unambiguously resolved by the photoluminescence enhancement.

The authors are grateful to Y. Lozovik and to L. Butov for a critical reading of the manuscript, and to M. Cristiani for stimulating discussions. F.D. and M.A. would also like to thank J. Eschner and M. Lewenstein for their support of this project. This work was supported partially by the the Spanish MEC (QOIT, CSD2006-00019; QNLP, FIS2007-66944) while F.D. also acknowledges the Ramón y Cajal program.

[1] Miesner H. J. et al., Science **279**, 1005 (1998)
[2] Bloch I, Dalibard J and Zwerger W., Rev. Mod. Phys. **80**, 885 (2008)
[3] Savvidis P. G. et al., Phys. Rev. Lett. **84**, 1547 (2000)
[4] Huang R., Tassone F., Yamamoto Y., Phys. Rev. **61**, (R)7854 (2000)
[5] Saba M. et al., Nature **414**, 731 (2001)
[6] Deng H. et al., Science **298**, 199 (2002)
[7] Kasprzak J. et al., Nature **443**, 409 (2006)
[8] R. Balili et al.,Science **316**, 1007 (2007)
[9] Moskalenko S. A. and Snoke D. W., *Bose-Einstein condensation of Excitons and Biexcitons* (Cambridge Univ. Press, 2000)
[10] S. Yang et al., Phys. Rev. Lett. **97**, 187402 (2006)
[11] Timofeev V. B. and Gorbunov A. V., Phys. Stat. Sol. (c) **7**, 2379 (2008)
[12] Lozovik Yu. E., Yudson V. I., J.E.T.P. **44**, 89 (1976)
[13] L.V. Butov, J. Phys.: Condens. Matter **16**, R1577 (2004)
[14] L.V. Butov, J. Phys.: Condens. Matter **19**, 295202 (2007)
[15] Hammack A.T. et al., J. Appl. Phys. **99**, 066104 (2006).
[16] Chen G. et al., Phys. Rev. B **74**, 045309 (2006)
[17] Gärtner A., Schuh D., and Kotthaus J. P., Physica E **32**,195 (2006)
[18] High A. A. et al., Phys. Rev. Lett. **103**, 087403 (2009)
[19] Remeika M. et al., Phys. Rev. Lett. **102**, 186803 (2009)
[20] Vögele X. P. et al., Phys. Rev. Lett. **103**, 126402 (2009)
[21] Butov L. V. et al., Phys. Rev. B **59**, 1625 (1999)
[22] Butov L. V. et al., Phys. Rev. Lett. **86**, 5608 (2001)
[23] Ivanov A. L., J. Phys.: Condens. Matter **16**, S3639 (2004)
[24] Rapaport R. et al., Phys. Rev. B **72**, 075428 (2005)
[25] Ben-Tabou de-Leon S. and Laikhtman B., Phys. Rev. B **63**, 125306 (2001)
[26] Schindler C. and Zimmermann R., Phys. Rev. B **78**, 045313 (2008)
[27] Laikhtman B. and Rapaport R., Phys. Rev. B **80**, 195313 (2009)
[28] Ivanov A. L., Europhys. Lett. **59**, 586 (2002)
[29] Zimmerman R., Runge E., Phys. Status Solidi A **164**, 511 (1997)
[30] High A. A. et al., Nano Letters **9**, 2094 (2009)
[31] Vörös Z. et al., Phys. Rev. Lett. **103**, 016403 (2009)
[32] Vörös Z., Snoke D. W., Pfeiffer L. and West K., Phys. Rev. Lett. **97**, 016803 (2006)
[33] Snoke D., Solid. Stat. Comm. **146**, 73 (2009)